Brain Research 1806 (2023) 148289

Contents lists available at ScienceDirect

Brain Research

journal homepage: www.elsevier.com/locate/brainres

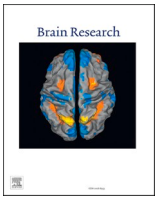

Individualised profiling of white matter organisation in moderate-to-severe traumatic brain injury patients

Adam Clemente [a,*], Arnaud Attyé [b,c], Félix Renard [b], Fernando Calamante [c,d], Alex Burmester [e], Phoebe Imms [f], Evelyn Deutscher [e], Hamed Akhlaghi [g,h], Paul Beech [i], Peter H Wilson [k], Govinda Poudel [j], Juan F. Domínguez D [e,1], Karen Caeyenberghs [e,1]

[a] *Neuroscience of Addiction and Mental Health Program, Healthy Brain and Mind Research Centre, School of Behavioural, Health and Human Sciences, Faculty of Health Sciences, Australian Catholic University, Melbourne, Victoria, Australia*
[b] *CNRS LPNC UMR 5105, University of Grenoble Alpes, Grenoble, France*
[c] *School of Biomedical Engineering, The University of Sydney, Sydney, New South Wales 2006, Australia*
[d] *Sydney Imaging – The University of Sydney, Sydney, Australia*
[e] *Cognitive Neuroscience Unit, School of Psychology, Deakin University, Geelong, Victoria, Australia*
[f] *Leonard Davis School of Gerontology, University of Southern California, Australia*
[g] *Emergency Department, St. Vincent's Hospital, University of Melbourne, Melbourne, Victoria, Australia*
[h] *Department of Psychology, Faculty of Health, Deakin University, Australia*
[i] *Department of Radiology and Nuclear Medicine, The Alfred Hospital, Melbourne, Victoria, Australia*
[j] *Mary MacKillop Institute for Health Research, Faculty of Health Sciences, Australian Catholic University, Melbourne, Victoria, Australia*
[k] *Development and Disability over the Lifespan Program, Healthy Brain and Mind Research Centre, School of Behavioural, Health and Human Sciences, Faculty of Health Sciences, Australian Catholic University, Melbourne, Victoria, Australia*

ARTICLE INFO

Keywords:
Diffusion MRI
TBI
Individualised Profiling
TractLearn: Personalised Medicine

ABSTRACT

Background and purpose: Approximately 65% of moderate-to-severe traumatic brain injury (m-sTBI) patients present with poor long-term behavioural outcomes, which can significantly impair activities of daily living. Numerous diffusion-weighted MRI studies have linked these poor outcomes to decreased white matter integrity of several commissural tracts, association fibres and projection fibres in the brain. However, most studies have focused on group-based analyses, which are unable to deal with the substantial between-patient heterogeneity in m-sTBI. As a result, there is increasing interest and need in conducting individualised neuroimaging analyses.
Materials and methods: Here, we generated a detailed subject-specific characterisation of microstructural organisation of white matter tracts in 5 chronic patients with m-sTBI (29 – 49y, 2 females), presented as a proof-of-concept. We developed an imaging analysis framework using fixel-based analysis and TractLearn to determine whether the values of fibre density of white matter tracts at the individual patient level deviate from the healthy control group (n = 12, 8F, M_{age} = 35.7y, age range 25 – 64y).
Results: Our individualised analysis revealed unique white matter profiles, confirming the heterogenous nature of m-sTBI and the need of individualised profiles to properly characterise the extent of injury. Future studies incorporating clinical data, as well as utilising larger reference samples and examining the test–retest reliability of the fixel-wise metrics are warranted.
Conclusions: Individualised profiles may assist clinicians in tracking recovery and planning personalised training programs for chronic m-sTBI patients, which is necessary to achieve optimal behavioural outcomes and improved quality of life.

* Corresponding author at: Healthy Brain and Mind Research Centre, Australian Catholic University, Level 3, 115 Victoria Parade, Fitzroy, Melbourne, VIC 3065, Australia.
E-mail address: adam.clemente@acu.edu.au (A. Clemente).
[1] Shared Senior Authors.

https://doi.org/10.1016/j.brainres.2023.148289
Received 3 November 2022; Received in revised form 22 December 2022; Accepted 15 February 2023
Available online 20 February 2023

1. Introduction

At least 27 million individuals worldwide sustain moderate-severe traumatic brain injuries (TBIs) annually that result in death or require hospitalisation (James et al., 2019). Interestingly, these moderate to severe TBIs (m-sTBIs) account for almost 20% of brain injuries globally and results in a heavy burden on healthcare systems (Dewan et al., 2019). Long-term outcomes after m-sTBI after often poor, with patients facing lifelong chronic symptoms (such as cognitive, motor, social and psychological deficits.) that are difficult to treat and predict (Dewan et al., 2019; Maas et al., 2022). The heterogeneity of the pathophysiology within m-sTBI is believed to be a key factor in why it is difficult to treat and predict recovery outcomes for individual m-sTBI patients (Dadas et al., 2018; Maas et al., 2022).

Numerous diffusion-weighted MRI (dMRI) studies have demonstrated that m-sTBI is associated with structural white matter changes in association/projection/commissural fibre bundles, which play an important role in long-term behavioural deficits (see reviews and meta-analyses; Roberts et al., 2013; Wallace et al., 2018). For example, one study revealed reduced fractional anisotropy (FA) values in 13 major white matter tracts (e.g., superior longitudinal fasciculus, genu of corpus callosum) in m-sTBI patients, compared to controls (Attyé et al., 2021). These reduced values of white matter organisation were associated with poor performance on a range of cognitive tasks (i.e., executive function, attention, and memory).

Most of our understanding how white matter is impacted in m-sTBI comes from group-based analyses, which fail to reflect changes at an individual level. However, this major focus on group-wise comparisons of dMRI metrics (i.e., *N* patients vs *M* controls) is starting to be questioned. A number of scholars regard individualised profiling (i.e., 1 patient vs *M* controls) as a promising response to the challenges posed by this heterogeneity (Attyé et al., 2021; Chamberland et al., 2021; Jolly et al., 2020; Lv et al., 2021). The goal of individualised profiling is to enhance the characterisation of brain alterations in individuals from clinically heterogeneous groups, rather than to just focus on how their patient cohort as a group departs from healthy controls.

One study investigated 45 white matter tracts in individual schizophrenia patients ($N = 322$) in comparison to a group of healthy controls ($N = 195$), revealing widespread but highly heterogeneous deviations in FA across all tracts (Lv et al., 2021). In addition, another study revealed a large degree of inter-individual variability in white matter microstructure abnormalities in children with copy number variants, highlighting the need for individualised profiles (Chamberland et al., 2021).

The above-mentioned studies do not focus on patients with TBI. However, heterogeneity in patient profiles is a hallmark characteristic of TBI and therefore should no longer be avoided or ignored (Maas et al., 2022). Recently, it has been suggested that by adopting new methodological approaches (such as single-subject analyses, normative modelling), we can account for this inherent heterogeneity in TBI specifically. Using single-subject analyses to its full potential for the first time, an example study was presented in Jolly et al. (2021), who compared 1 patients vs a reference control group. Through this methodology, they examined diffuse axonal injury (DAI) in individual patients with TBI using the dMRI tensor-based metric fractional anisotropy. This study revealed for the first time the importance of (1) moving beyond conventional scans for axonal injury diagnosis as diffuse injuries may not be evident on conventional scan sequences and; (2) individualised profiling of m-sTBI patients due to large heterogeneity seen within patients. Focusing only on differences in group means obscures between-patient heterogeneity in the topography of the lesions, type of lesion, tissue repair and recovery mechanisms, limiting our understanding of the aetiology of TBI and identification of effective rehabilitation and treatment (Verdi et al., 2021).

To the best of our knowledge, only three studies so far have performed single-subject analyses in TBI patients (Attyé et al., 2021; Jolly et al., 2020; Poudel et al., 2020). One study conducted a subject vs reference group (i.e. healthy controls) analysis for the identification of traumatic axonal injury in individuals with m-sTBI (Jolly et al., 2020). They revealed substantial heterogeneity in tensor-based metrics (e.g., FA) across m-sTBI patients. Another study introduced a novel data-driven learning framework called TractLearn for quantitative analysis of white matter tracts (Attyé et al., 2021). TractLearn overcomes limitations of the standard subject-versus-reference-group studies, because it uses controls variability as normative reference instead of computing average values of the dMRI metrics of controls as reference scores. Using TractLearn, this research detected abnormal voxels in a wide array of white matter tracts using both tensor (e.g., FA) and constrained spherical deconvolution-based (e.g., apparent fibre density, AFD) metrics in five mild TBI patients[4]. Their findings illustrated the ability of TractLearn to capture both the variability of the healthy controls ($N = 20$) and the subtle quantitative alterations in a brain bundle at the voxel scale in mild TBI patients, all of which did not show visible lesions on standard MRI scans.

In the present study, our overall aim is to implement TractLearn in m-sTBI patients with visible focal lesions. We consider TractLearn over classical voxel-to-voxel methods since this method can model the bundle's variability better and at the single-subject level (Attyé et al., 2021). The aim of the current study is to demonstrate a proof-of-concept of a framework framework for generating subject-specific brain profiles of our m-sTBI patients in the chronic stage of injury. We define brain profiles as profiles of brain imaging measures at the level of the individual patient (Scarpazza et al., 2020). We use advanced processing pipelines to derive different brain metrics to quantify subject-specific changes (e.g., white matter organisation; connectome network properties in our recent paper – Imms et al., 2022) and locate these brain profiles relative to a reference cohort. This contextual information enables us to meaningfully, qualitatively, and quantitatively, assess brain damage in single individuals. These resulting single-subject brain profiles can provide quantitative support and be used by clinicians to the classification of neuropathology types. These brain profiles may assist clinicians in formulating a neuroscience-guided integrative rehabilitation program tailored to individual TBI patients in the future. To this end, we will utilise the TractLearn framework to determine whether fibre density (FD) values derived from fixel-based analysis (FBA) (Raffelt et al., 2015, 2017) of white matter tracts of an individual patient deviate from a healthy reference group (N = 12). We have chosen FBA over the traditional diffusion tensor approach (as was done in previous research Jolly et al., 2020), as FBA offers greater specificity (Dhollander et al., 2021; Raffelt et al., 2012; Liang et al., 2021; Mito et al., 2018).

2. Materials and methods

2.1. Participants

m-sTBI participants were recruited at St Vincent's Hospital (H.A.) in Melbourne. Inclusion criteria included: (1) age range 18–65 years; (2) diagnosed with m-sTBI at the time of injury based on: (i) a Glasgow Coma Scale score between 3 and 12 (Teasdale & Jennett, 1974) (ii) loss of consciousness longer than 30 min; (iii) Post traumatic Amnesia (PTA) longer than 24 h (Rabinowitz and Levin, 2014) and; (iv) positive findings of gross injury on MRIs as per evaluation by a neuroradiologist (PB); (3) in the chronic phase (>6 months after injury); (4) ambulant or independently mobile at the time of recruitment; (5) no known diagnosed TBI prior to current brain injury and; (6) right-handed as defined by the Edinburgh Handedness Inventory (Oldfield, 1971).

A total of six patients with m-sTBI were recruited for this study. See Table 1 for a summary of demographic, injury, and clinical characteristics for the m-sTBI participants. The patients were compared to a reference group of 12 healthy controls (HC; age range = 25 – 64 years; $M_{age} = 35.70 \pm 11.4$ years; 8 females). This reference group enabled us to meaningfully assess the extent to which each individual TBI patient departed from the HC group in terms of fibre density metrics. Healthy

Table 1
Summary of Demographic, Injury, and Clinical Characteristics of the six m-sTBI Participants.

Participant ID	Age (years, months)/ sex	Time since injury (years, months)	Cause	MRI scan at time of testing, Lesion location / pathology	DAI Grade[1]	SPRS (total)[2]
TBI1	45, 3 M	21, 0	Car accident	Small area of encephalomalacia in the (R) precentral gyrus	0	48
TBI2*	49, 10 M	15, 6	Motor bike accident	Large areas of encephalomalacia involving (L, R) anterior and inferior frontal lobes, (R) lateral temporal lobe and (R) parietotemporal region extending to the (R) posterior frontal lobe. Focal T1 hypointensities in the anteromedial aspect of the (L) thalamus. Volume loss and T1 hypointensity on the anterior body and genu of the corpus callosum.	2	30
TBI3	49, 8F	3, 8	Horse riding accident	Bilateral anterior and inferior frontal encephalomalacia, (R) greater than (L), and (R) anterior temporal encephalomalacia. Small deep white matter T2 hyperintensities medial (R) parietal lobe. Small focal T1 hypointensity in the anterior body of the corpus callosum.	2	31
TBI4	29, 5F	15, 6	Horse riding accident	Bilateral inferior frontal and (L) anterior temporal encephalomalacia. Small area of encephalomalacia (L) superior frontal gyrus. (R) frontal burr hole with underlying ventricular drain tract.	0/1	34
TBI5	50, 2 M	18, 1	Car accident	Two small nonspecific deep white matter T_2 hyperintensities in the (R) parietal lobe (within normal limits for age).	0	51
TBI6	29, 7F	5, 10	Horse riding accident	Small T_1 hypointensity in splenium of corpus callosum. Scattered punctate T_2 hyperintensities in both cerebral hemispheres (approx. 6).	2	44

[1]Grading of Diffuse Axonal Injury (DAI) in accordance with a published grading syste[m] (Adams et al., 1989): a "0" grade indicates no confirmed DAI present; "1" is considered evidence of axonal injury in the white matter of the cerebral hemispheres, the corpus callosum, the brainstem and, less commonly, the cerebellum; "2" presence of a focal lesion in the corpus callosum; and "3" is interpreted as presence of a focal lesion in the dorsolateral quadrant or quadrants of the rostral brainstem. Anatomical T1-weighted image MRI scans were inspected and classified by an experienced neuroradiologist (P.B.) providing the descriptions of the lesions and DAI grading. [2] The Sydney Psychosocial Reintegration Scale (SPRS) measures psychosocial functioning in three domains of participation (Tate, Simpson, Soo, & Lane-Brown, 2011). These three domains are (i) occupational activity (i.e. work and leisure), (ii) interpersonal relationships, and (iii) independent living skills. Scores result from the sum of all questions and range from 0 to 52 for the overall scale, with higher scores indicating greater psychosocial functioning. * Subject excluded from analysis due to excessive motion. Abbreviations: M = male; F = female; L = left; R = right.

controls were recruited via social contacts and were included if they met the following criteria: (1) age range 18–65 years; (2) no history of neurological or psychiatric disorders; (3) right-handed as defined by the Edinburgh Handedness Inventory scale (Oldfield, 1971); ($M = 9.92$ $SD = 0.28$). Patient TBI2 was excluded from the analyses, due to severe head motion in the diffusion MRI data, therefore the final number of participants for this study was five. Written informed consent was obtained from each participant in accordance with the Helsinki declaration, and ethical approval was obtained by the St Vincent's Hospital Human Research Ethics Committee (#250/17).

2.2. MRI acquisition

Structural MRI scans were acquired on a 3 T Siemens PRISMA scanner with a 64-channel head coil at Murdoch Children's Research Institute in Melbourne, Australia. Single shell diffusion-weighted imaging was acquired using single-shot echo planar with twice-reinforced spin echo and a multi-band acceleration factor of 2 which was obtained with 70 contiguous transverse slices (FOV = 260 × 260 mm^2, voxel size = 2.3 mm isotropic, TR = 3500 ms, TE = 67 ms, A≫P, and TA = 6 min 17 s. A high angular resolution diffusion imaging (HARDI; Frank, 2001) gradient scheme was applied in 64 non-collinear gradient directions, maximum b-value of 3000 s/mm^2, and seven interleaved b0 images. A pair of anterior–posterior (AP) and posterior–anterior (PA) reverse phase-encoded images were also collected to correct for geometric distortions (TA = 50 s each).

Anatomical MRI scans were also acquired using a T_1 weighted imaging (ADNI) protocol with 104 contiguous sagittal slices (A≫P, FOV = 220 × 220 mm^2, voxel size = 1.0x1.00x1.50 mm^3, TR = 2250 ms, TE = 3.07 ms, flip angle = 9°, and TA = 5.48 min). These MRI scans were inspected and classified by an experienced neuroradiologist (P.B.) providing an overall description of the pathology as well as a DAI grade using a published grading system (as can be seen in Table 1; Adams et al., 1989).

2.3. MRI data processing

The current study uses a state-of-the-art processing pipeline which inherently deals with large focal lesions in m-sTBI patients (Dhollander et al., 2021). See (Fig. 1) for a schematic overview of the pipeline. Following the figure will be a detailed description of this processing pipeline.

2.3.1. Quality assessment of raw diffusion data

Prior to analysing the dMRI data, a rigorous quality analysis was conducted using ExploreDTI (v4.8.5; Leemans et al., 2009) which helped (1) detect potential mistakes which may have occurred when acquiring the data; and (2) identify and eliminate artefacts. Once the dMRI scans were acquired, raw folders were inspected to detect if the correct number of volumes had been acquired. This was the first step to ensure that the data had been acquired correctly. Following this, the quality of the data was inspected with ExploreDTI through three major steps. First, "looping" through each of the raw diffusion weighted images was utilised to detect any major movements throughout each participant scans. Following this, a colour coded FA map of the raw diffusion weighted images was checked to ensure that the direction of the colours were correct (i.e., left–right: red, inferior-superior: blue, anterior-posterior: green). Next, average residuals and outlier profiles per diffusion weighted image were checked to reflect the fit of the diffusion tensor. All participants passed the quality analyses and the data was ready for further analyses.

2.3.2. Pre-processing

MRI data was processed using MRtrix3Tissue (https://3Tissue.github.io), a fork of MRtrix3 (Tournier et al., 2019). The pre-processing steps included: denoising (Veraart et al., 2016), removal of Gibbs ringing (Kellner et al., 2016), and eddy current, motion, and susceptibility induced distortion correction with outlier replacement (Andersson and Sotiropoulos, 2016; Andersson et al., 2016). The pre-processed diffusion weighted images were then upsampled from 2.3 mm to 1.33 mm isotropic voxels before the computation of the upsampled brain masks. Data was upsampled as per the MRtrix FBA documentation (see https://mrtrix.readthedocs.io/en/0.3.16/workflows/fixel_based_analysis.html) as this can increase anatomical contrast and inherently improve downstream normalisation and statistics derived from the data (Dyrby et al., 2014).

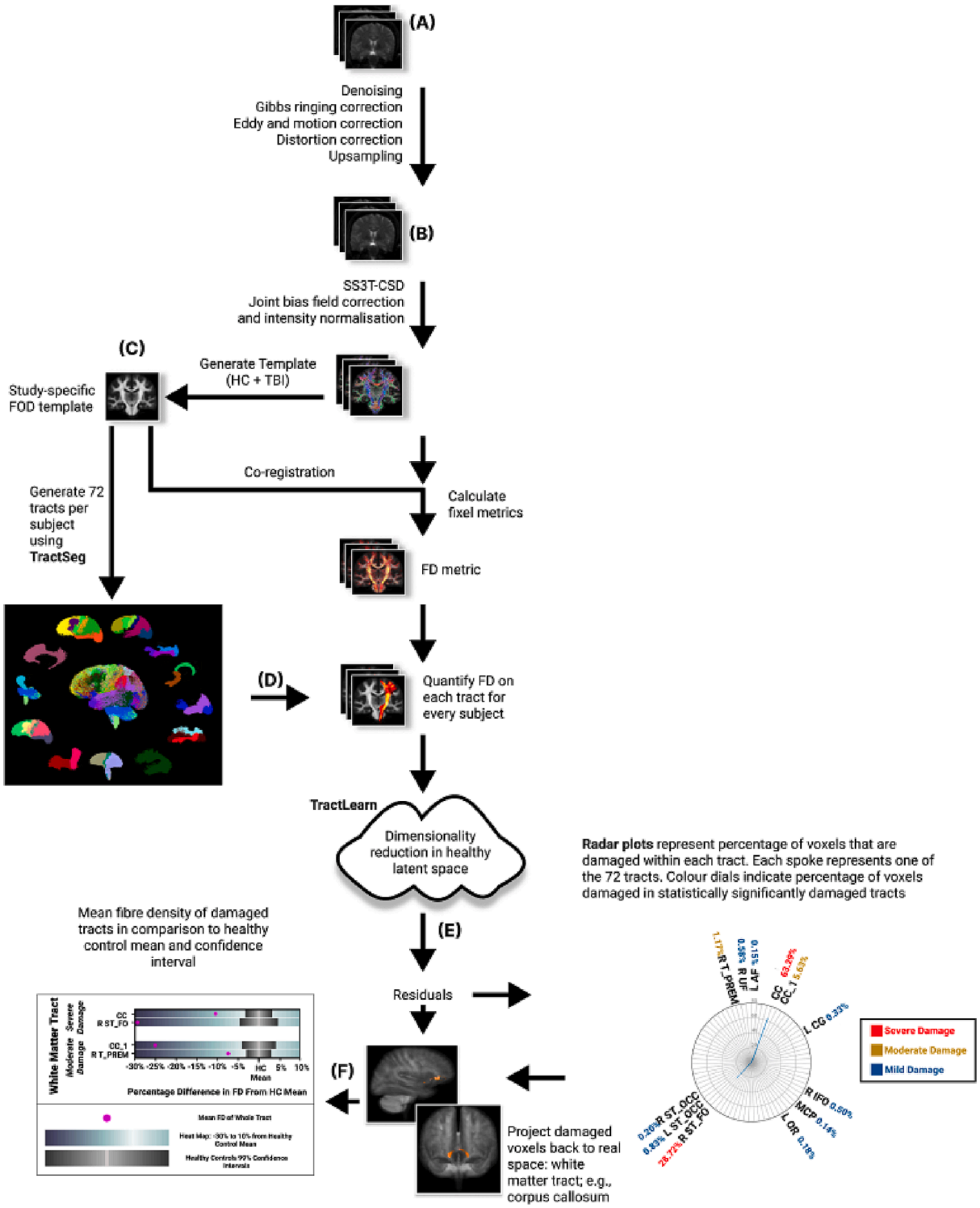

Fig. 1. Schematic overview of dMRI framework (A) Raw diffusion images were pre-processed to remove artefacts (noise, Gibbs-ringing, eddy/motion and geometric distortion). (B) Single shell 3-tissue constrained spherical deconvolution was then performed on the pre-processed images followed by joint bias field correction and intensity normalisation. (C) A study-specific population template was then constructed using HC (cross-sectional data) and m-sTBI patient data. (D) For each HC and m-sTBI participant, 72 tracts were generated using TractSeg and fixel-wise fibre density (FD) was computed for each individual tract. (E) TractLearn (which employs a manifold learning approach), was then used to detect abnormal voxels in fibre density for the m-sTBI patients when compared to the healthy controls. The results are illustrated in radar plots, which show the percentage of damaged voxels, and back-projections of damaged voxels in population template space are finally computed. (F) Heat maps of the mean FD of damaged tracts in relation to the mean FD of each tract of the healthy control group.

2.3.3. Fibre orientation distribution calculation

As our m-sTBI patients had large focal lesions, a robust pipeline was needed to control for this. We estimated the fibre orientation distributions (FOD) estimations using single-shell 3-tissue constrained spherical deconvolution (SS3T-CSD; Dhollander and Connelly, 2016). Research on patients with lesions in both MS (Gajamange et al., 2018) and stroke (Egorova et al., 2020; Gottlieb et al., 2020) have computed white matter FODs using SS3T-CSD which is suggested to be the best current method for dealing with lesions (Dhollander et al., 2019; Dhollander et al., 2016; Dhollander et al., 2021). Following this, we performed joint bias field correction and global intensity normalisation (Raffelt et al., 2015).

2.3.4. Fibre orientation distribution template construction

We generated a study specific unbiased FOD template using the FOD templates from the (1) five m-sTBI participants and; (2) the 12 cross-sectional HC participants, using linear and non-linear registration of the FOD image (Raffelt et al., 2011; Raffelt et al., 2012). This method for template construction is used in other studies profiling single-subjects (Attyé et al., 2021) and is recommended on the MRtrix3 documentation (https://www.mrtrix3.org). This was followed by the registration of each FOD image to template space (Dhollander et al., 2021). FOD segmentation was then performed to compute fixels at both template-level and individual-level (Raffelt et al., 2015; Raffelt et al., 2017). Finally, fixels at individual-level were all reoriented to the corresponding fixels of the FOD template in order to conduct group comparisons of fixel-wise metrics (Raffelt et al., 2011).

2.3.5. Fibre density calculation

Based on the 2 million tractograms, the FD fixel-metric was calculated in template space for each individual participant as we are interested in microstructural changes of the white matter (Raffelt et al., 2015). For the TractLearn tool, FD was converted to voxels in order for the toolbox to run as it requires a specific form of quantitative data. These statistics were utilised for further analyses.

2.3.6. Tracts of interest construction

We used the automated TractSeg tool to delineate 72 tracts for the individualised profiles (Wasserthal et al., 2018, 2019). TractSeg is a novel semi-automated probabilistic tractography tool that directly segments streamlines from tracts in the field of fibre orientation distribution function peaks without using common time consuming techniques, such as tractography, image registration, or parcellation (Wasserthal et al., 2018). With this, TractSeg provides fast and accurate segmentation of 72 white matter tracts, providing a good balance between manual delineation and automated atlas-based tracking approaches (Wasserthal et al., 2018). Specifically, TractSeg was applied to the study-specific FOD population template to delineate the 72 tracts for the individualised profiles.

We conducted rigorous visual quality check inspections of the data. Firstly, we visualised the reconstructed tracts derived from TractSeg in individual space to check that all 72 tracts were not delineated in regions of lesioned tissue. Following this, similar to recent applications of this toolbox using FBA, for each individual participant, we warped the tracts from subject space into a common population template space to be able to compare metrics along each tract more robustly (Attyé et al., 2021; Genc et al., 2020). Importantly, we performed a QA check of all tracts for each individual patient within the template space to ensure that all tracts were anatomically representative. All tracts were generated using the default TractSeg pipeline for each individual participant at each time point using their individual white matter FODs which were then warped into population template space (https://github.com/MIC-DKFZ/TractSeg), apart from upgrading each tract from the default 2000 to 10,000 streamlines. These tracts were used for further analyses.

2.4. Individualised profiling statistical analysis

To develop individualised profiles, our analysis was two-fold. This is presented as a proof-of-concept. First, we used the TractLearn toolbox (Attyé et al., 2021) (https://github.com/GeodAIsics/TractLearn-WholeBrain) to identify damaged white matter tracts from the 72 tracts delineated via TractSeg (Wasserthal et al., 2018, 2019. For a given dMRI metric, TractLearn detects abnormal voxels for each tract in every patient by using a manifold learning approach to determine which voxels deviate from normative healthy control measures (Attyé et al., 2021). A Z-score is applied to all voxels in each tract, which indicates a difference in the dMRI metric between a patient and the control group. Bonferroni correction for multiple comparisons (given by the size of the tract in number of voxels) is then applied. The remaining voxels are considered statistically significantly damaged. The percentage of damaged voxels thus identified within each tract is then computed. In this paper, we used the fixel-wise fibre density (FD) metric. TractLearn therefore provided us with an estimate of the extent of damage in FD at the subject level for each of our patients. We categorised the severity of the extent of damage of FD for each tract as either “severe” (>10% damaged voxels), “moderate” (1–10% damaged voxels), or “mild” (<1% damaged voxels). Please note, these are arbitrary labels of damage severity based on damaged tracts seen in mild, moderate, and severe TBI (Wallace et al., 2018). For visualisation, these damaged voxels were then projected back to population template space. (See Fig. 2 for an example radar plot and the full list of abbreviations of tracts).

In the second analysis, for every individual patient, we calculated the mean FD of each whole tract that was moderately or severely damaged (as quantified by TractLearn in the previous step). FD was also calculated for the reference HC group to generate reference points for comparisons against each individual TBI patient. We then estimated the 99% confidence intervals (CIs) and the mean FD of each tract for the HC group. Subsequently, we classified the profiles of the patients in line with previous normative work (Lv et al., 2021), whereby FD of the tract of the patient is classified as either “normal” (if the FD value of the tract falls within the 99% CI of the HC), “supra-normal” (greater than the 99% CI of the HC), or “infra-normal” (lower than the 99% CI of the HC). This provides an overall measure representative of FD loss in tracts relative to controls.

3. Results

Patient TBI1 presented with the highest number of injured tracts (39 tracts; 3 severe, 18 moderate, 18 mild), most notably in the corpus callosum (segments 1, 4, 5 - moderate), thalamo postcentral (severe), fornix (severe), and CST (moderate), with some of the tracts including at least 10% damaged voxels. When assessing whole tract FD, we observed between 10 and 35% FD loss, relative to the HC mean, in infra-normal tracts. Interestingly, despite having a low DAI grade (score of 0 on the Adam’s system), patient TBI1 presented with moderate damage not visible on conventional scanners. Finally, despite a wide array of damaged tracts, patient TBI1 self-reported a high psychosocial functioning since their injury on the Sydney Psychosocial Reintegration Scale (SPRS).

TractLearn results for patient TBI3 showed a significant number of damaged voxels (12 tracts: 2 severe, 2 moderate, 8 mild). The moderately and severely damaged tracts, include the whole corpus callosum (severe), segment 1 (rostrum) of the corpus callosum (moderate), right thalamo-premotor (moderate), and right striato-fronto-orbital tract (severe). All these tracts were also found infra-normal in terms of whole tract FD, with an 8 to 30% FD loss, relative to the reference group. Despite having a moderate to severe diffuse axonal injury grade (score of 2 on the Adam’s system), patient TBI3 presented with damage to 16% of the 72 tracts examined, with most of them mildly damaged. Also, patient TBI3 self-reported a moderate psychosocial functioning since their injury on the SPRS which showed correspondence with their relatively

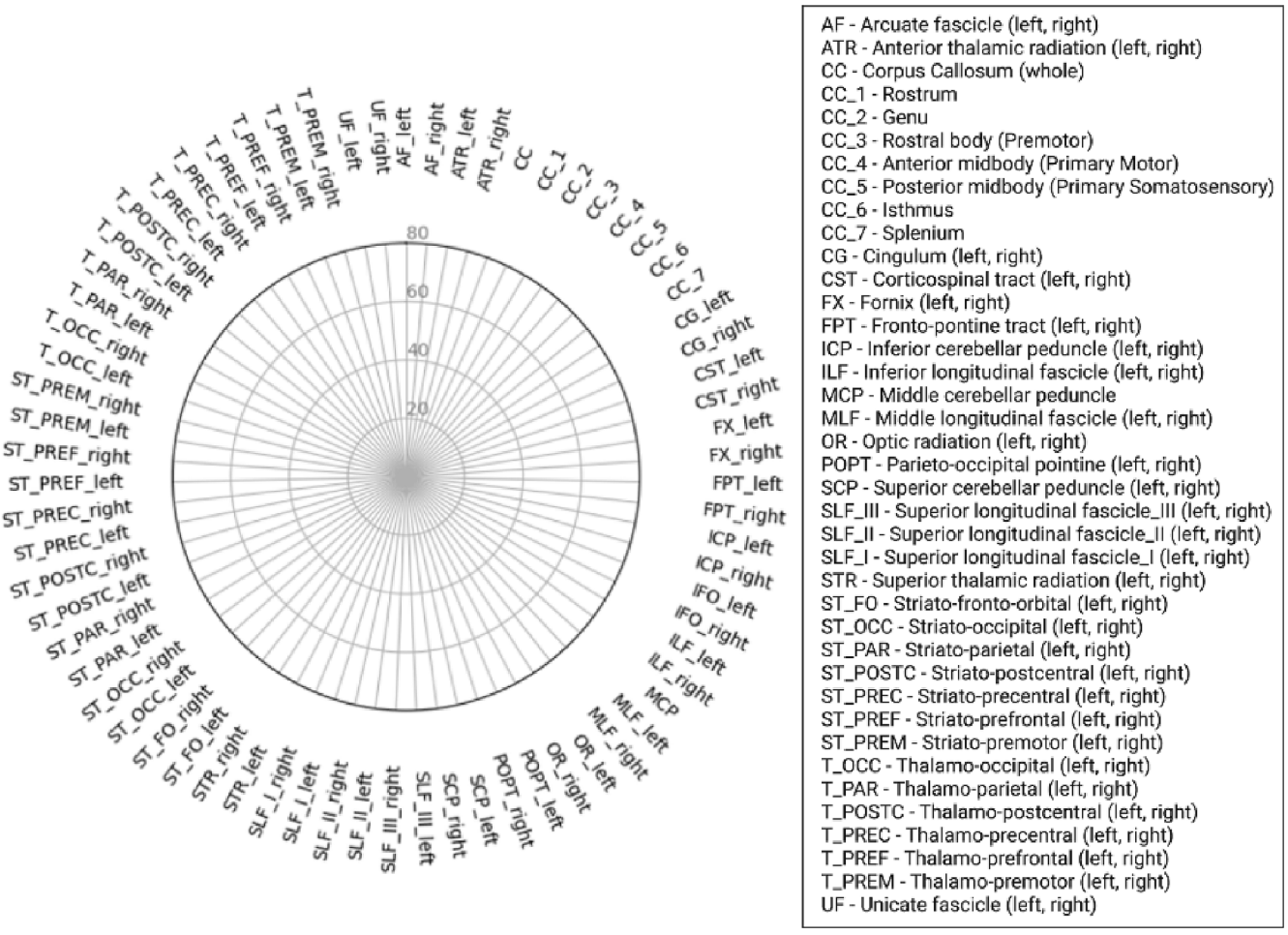

Fig. 2. Example TractLearn radar plots for damaged tract profiles alongside the full list of abbreviations of tracts as described and delineated through TractSeg. Numbers in the plots represent percentage of voxels within tract that is damaged.

low number of damaged tracts.

As per the radar plot for patient TBI4, this patient showed a higher number of damaged voxels in 8 tracts, including the corticospinal tract, bilaterally (mild), fornix (severe), right anterior thalamic radiation (mild), corpus callosum (whole CC, moderate), left fronto-pontine tract (mild), and left striato-occipital tract (mild). The corpus callosum and fornix showed an infra-normal 10–20% FD decrease relative to controls. Patient TBI4 showed overlap between the diffuse axonal injury grade (score of 0/1 on the Adam's system) and the limited number of damaged tracts detected. Patient TBI4 also self-reported moderate psychosocial functioning since their injury on the SPRS, which aligned with a small percentage (i.e., 11%) of significantly damaged tracts.

The TractLearn results for patient TBI5 revealed a high number of voxels with significant altered FD in 20 white matter tracts, including the corpus callosum (whole CC moderate damage, mild damage in segments 5–7), optic radiations (mild to moderate damage), striato-occipital bundles (mild-moderate damage), corticospinal tract (moderate) and thalamic post central bundles (moderate). Except for the right thalamic postcentral bundle, the moderate-and-severely damaged tracts can be classified as infra-normal (5–30% FD loss). Interestingly, despite the low diffuse axonal injury grade (score of 0 on the Adam's system), patient TBI5 presented with a wide array of mild damage not visible on conventional scanners. In addition, patient TBI 5 self-reported high psychosocial functioning since their injury on the SPRS despite 28% of tracts showing at least mild damage.

Patient TBI6 presented only with damaged voxels in the left striato-occipital fibre bundle (mild). Example TractLearn radar plots are presented in (Fig. 2), and FD heatmaps are presented in (Fig. 3). In addition, the back projections of moderate to severely damaged tracts allowed to identify the location of altered voxels within each bundle using FD, as illustrated in (Fig. 4) for TBI1 and TBI3 patients. Despite having a moderate to severe diffuse axonal injury grade (score of 2 on the Adam's system), patient TBI6 presented with moderate damage in only 1/72 tracts. Also, TBI6 self-reported relatively high psychosocial functioning since their injury on the SPRS which aligns with the limited number of damaged tracts,Fig. 5.

4. Discussion

The present study provides a proof-of-concept study of TractLearn in five patients with m-sTBI to characterize patient-specific FD loss patterns in comparison to healthy controls. These results provide further evidence of the benefits of characterising abnormalities at the patient level when dealing with highly heterogeneous populations. First, we will discuss our observations from these individualised profiles followed by discussion of key ideas to improve individualised profiles of tract-specific white matter.

4.1. Individualised profiling of white matter microstructure

The individual profiles showed substantial variation across participants, ranging in number from one damaged tract in one patient (i.e., patient TBI6) to 39 damaged tracts in another (i.e., patient TBI1). The secondary analysis of tract-wide FD provides further insights into the

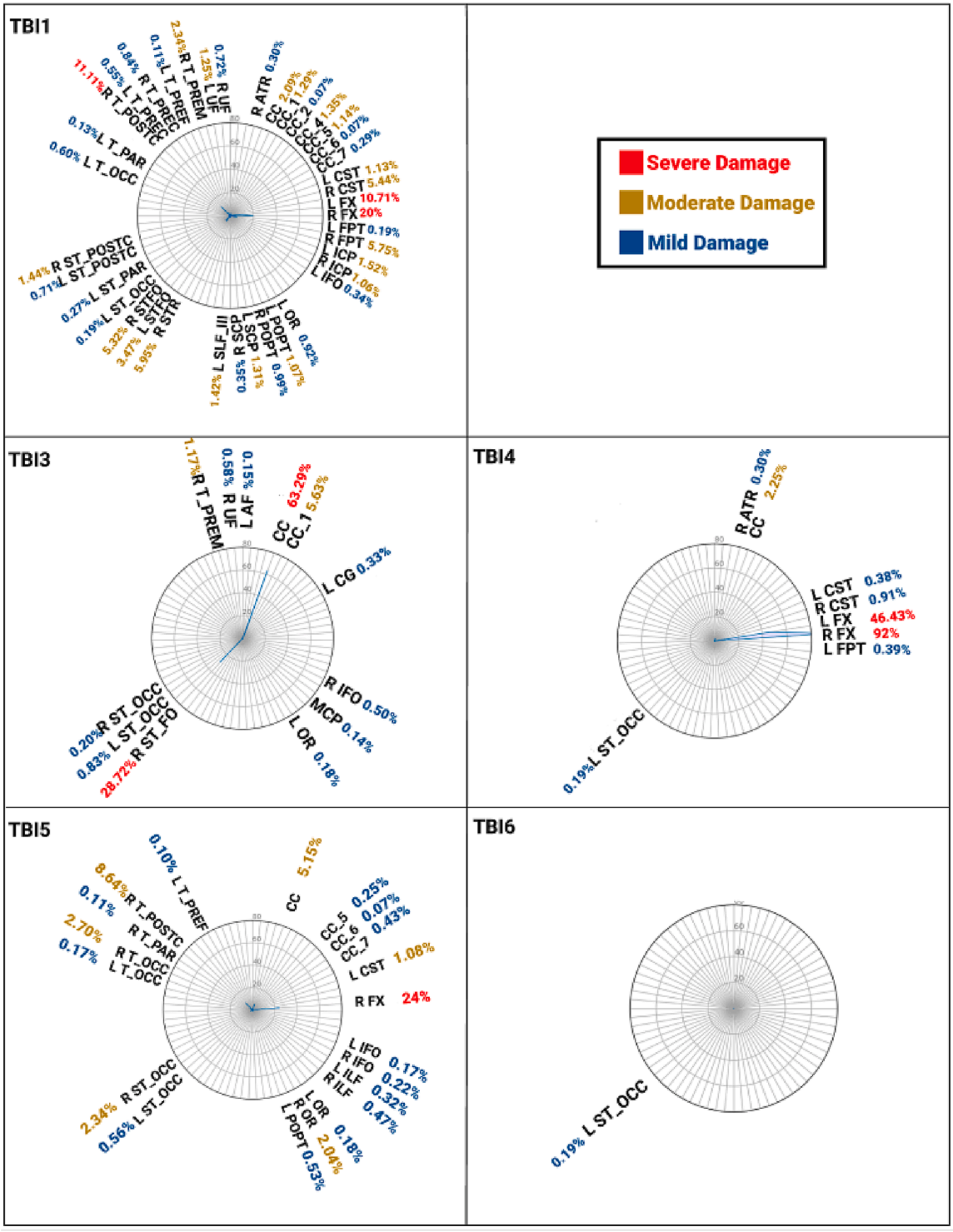

Fig. 3. TractLearn profiles of all m-sTBI patients, presenting the percentage of damaged voxels of FD in various tracts using TractLearn. Numbers of damage denote the severity of the damage; blue = mild, yellow = moderate, red = severe.

highly heterogeneous damage across m-sTBI patients. First, this analysis revealed up to nearly 40% tract-wide FD loss in patients relative to controls. Moreover, inspection of the heatmaps vis-à-vis the radar plots show that the extent of statistically detectable (by TractLearn), localised damage is not the whole story: tracts relatively spared in terms of extent of damage, may still exhibit a sizable amount of FD loss when considered as a whole. In the most salient case, the left uncinate fasciculus in patient TBI1 exhibited close to 40% FD loss tract-wise; however, the extent of damage to this tract was only 1.25%. This may mean a tract-wise loss of FD not detectable at the voxel level and/or a very substantial FD loss in the voxels detected as damaged that disproportionally affected the tract-wise metric. TractLearn and the tract-wide analysis therefore offer complementary information necessary to more fully characterise the damage sustained by white matter tracts. Together, these results highlight the variability and heterogeneity that is intrinsic to m-sTBI patients, which is consistent with reports from previous group-based studies (Han et al., 2017; Strangman et al., 2010; Verhelst et al., 2019).

On the other hand, there were tracts which seem to be more

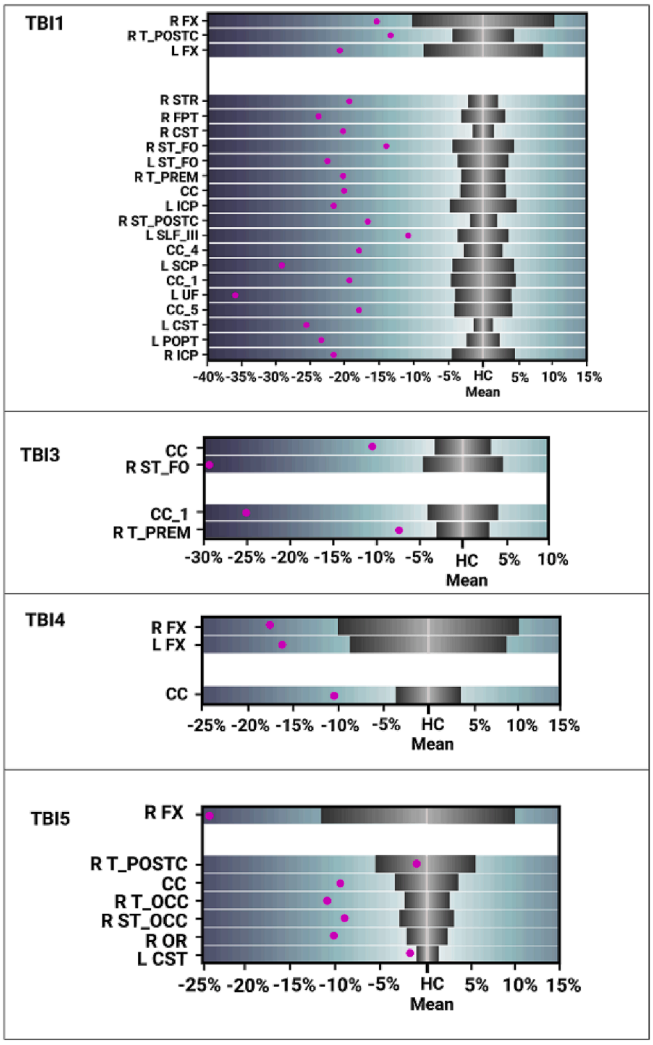

Fig. 4. Fibre density (FD) heatmaps of m-sTBI patients. Each heatbar shows the mean FD of the severe (top panel) and moderately (bottom panel) damaged tracts. Tracts are listed from the highest number of damaged voxels to the lowest. For each heatmap, the X-axis represents the percentage difference in FD from the healthy control mean. Grey heat maps in the centre represent the 99% healthy control confidence intervals.

frequently vulnerable as they were damaged across multiple participants. They include various segments of the corpus callosum (CC), the fornix as well as thalamo-postcentral tracts. This is in line with previous research (Wallace et al., 2018; Caeyenberghs et al., 2011). Studies utilising tensor-based metrics, for example, showed the CC as a vulnerable tract to long-term damage following m-sTBI[26]. This is common in m-sTBI patients in the chronic phase, who are prone to neurodegeneration of the white matter (Poudel et al., 2020), most likely as a result of secondary injury mechanisms, such as (Wallerian) degeneration (Koliatsos and Alexandris, 2019). In addition, the sensitivity of the CC for m-sTBI impact may also be explained by the anatomy of this tract which is ideal for the tensor model, subsequently leading to a better fit, a lower contribution of noise to the diffusion estimations and higher statistical power (Dennis et al., 2021).

Finally, 3 out of the 5 patients showed overlap between the SPRS clinical outcome measure and the damage observed in the white matter tracts detected by TractLearn. The SPRS measures the extent to which a patient's lifestyle may have changed as a result of an acquired brain injury and is a valid measure for monitoring chronic outcomes many years post-TBI (Tate et al., 2011). This provides preliminary evidence of interpretability of these individualised profiles and clinical outcomes in

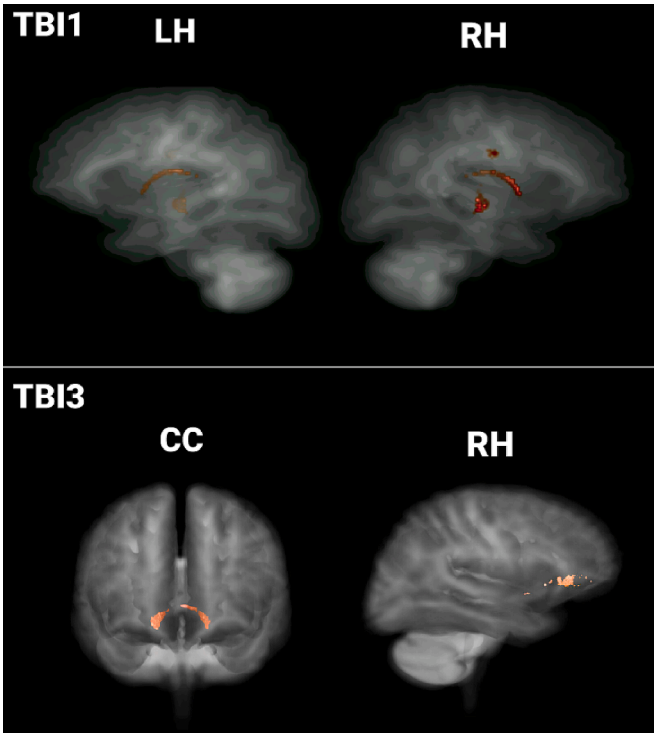

Fig. 5. Back-projection visualisations of TBI1 and TBI3, showing the damaged voxels of the severely damaged tracts projected back into population template space. LH = left hemisphere; RH = right hemisphere, CC = corpus callosum.

chronic TBI patients, but also highlights the heterogeneity seen across individual patients.

4.2. State-of-the art processing pipeline and implications of single-subject profiling

Our patients presented large focal lesions, representative of m-sTBI. However, using single-shell 3 tissue constrained spherical deconvolution (SS3T-CSD; Dhollander and Connelly, 2016; Dhollander et al., 2019), we were able to reconstruct the majority of the white matter tracts in a robust manner. This approach utilises group-average response functions for white matter, grey matter, and cerebrospinal fluid tissue types (Dhollander and Connelly, 2016; Dhollander et al., 2016). These response functions are tissue-specific signal models that allow tissue signal fraction estimation of grey matter and cerebrospinal fluid signals as well as white matter fibre orientation distributions (FODs) through spherical deconvolution analysis. This makes it possible to clearly delineate white matter fibre-bundles for TractLearn analysis. Computing white matter FODs using SS3T-CSD has previously been suggested as being able to inherently deal with lesions (Dhollander et al., 2021; Egorova et al., 2020; Gajamange et al., 2018; Gottlieb et al., 2020).

In addition, we also performed whole brain analysis at baseline through the use of TractSeg utilising the fibre-specific FD metric from the FBA framework, which overcomes drawbacks of tensor-based metrics (i.e., modelling crossing fibres) used in previous studies[6]. In advanced analyses, control for subject motion is essential, an issue that can be of particular importance in TBI patients, who can be less cooperative during MRI scanning. Motion control be achieved through patient preparation in a dummy scanner, online tracking of motion during scanning and re-running the protocol if excessive motion is detected.

TractLearn was used to detect damaged tracts, which relies on a manifold learning approach[4]. This framework (as opposed to deep-learning methods) for single-subject anomaly detection has two advantages over classic statistics methods:

1. Decreasing the number of false positive findings by capturing the anatomical variability and contrast variation from the healthy atlas. A benefit of manifold learning (compared with deep learning) is that it does not rely on the need of large number of subjects, which makes it useful for studies like the present one and for clinical translation. However, future studies will benefit from using larger control reference groups ($N > 50$).
2. Decreasing the number of false negatives by providing a nonlinear global analysis of all voxels in brain bundles, as opposed to a classic statistical method where all voxels are analysed independently.

Also, a benefit of this approach is that it does not require an explicit mask (which is very time consuming) and can operate over damaged tissue. This leads to not having to exclude subjects from analyses - an issue which has plagued research in populations with large lesions, with implications for representativity. Overall, our study indicates that this advanced method of lesion detection can identify extensive fibre bundle damage in TBI patients in comparison with previous individualised profiling methods. However, in the absence of a gold-standard (i.e., a procedure that is widely accepted for clinical use), it is difficult to precisely ascertain its accuracy.

4.3. Limitations and future studies

There are some limitations in this study that should be considered for future research. As mentioned earlier, future studies with larger sample sizes are needed (Jolly et al., 2020; Lv et al., 2021), a key limitation of this study are the low sample sizes of our TBI group and reference group. Our results need to be validated using control and TBI samples that are large enough to capture the normal variability (age and sex effects) and pathological variability white matter organisation. Also, although research demonstrated high test–retest reliability for TractSeg and TractLearn (Attyé et al., 2021), future studies should examine test–retest reliability across different scanners (vendor, software, strength) and data acquisition (Grech-Sollars et al., 2015; Karayumak et al., 2019; Mirzaalian et al., 2016; Schmeel, 2019; Tax et al., 2019). Continuing improvements in multi-site scanner harmonisation procedures will offer the possibility of increasing data from healthy cohorts from different scanning sites that can serve as reference which will increase the precision of the single-subject analyses (Liew et al., 2022; Olsen et al., 2021). Continued improvement in cross-scanner harmonisation is essential for the feasibility of this framework to ensure that large control cohorts are not required at each scanning facility – enabling feasibility of this process in terms of costs and clinical accessibility (Olsen et al., 2021).

Our study only utilised T1 images for DAI grading and lesion identification. In future studies, it is important to use other structural imaging modalities such as fluid attenuated inversion recovery (FLAIR) and susceptibility weighted imaging (SWI) for best practice guidelines for DAI grading and lesion identification (Olsen et al., 2021). This may be a reason for the lack of consistency between the DAI grades and TractLearn results. However, this study did employ the use of expert raters using hospital-level classification techniques through the use of an established procedure (Adams et al., 1989), still, DAI grading remains subjective with these processes and there is no general consensus regarding for the best classification type across the field (Jolly et al., 2020; Volovici et al., 2021). In addition, alternative MRI location-based grading scales (such as the modified Adams-Gentry system) may perform better than the Adams Grading system for the DAI despite its relevance as an established method (Volovici et al., 2021). The Adams Grading system for the DAI is not usually used for MRI as it is a pathological based system – this may also account for lack of consistency found between DAI grading and TractLearn results. This study highlights the importance of alternative DAI grading classifications as discussed in recent papers and the push toward consensus in the field (Jolly et al., 2020; Volovici et al., 2021).

In addition, longitudinal profiles need to be developed and validated to track the progression of damaged tracts over time or after a specific training program. Conducting TractLearn in a longitudinal analysis is possible and has the potential to overcome these drawbacks. The next key important step is to incorporate behavioural data to further understand the clinical relevance of structural changes in the white matter in TBI patients. Although the purpose of this study was to validate the neuroimaging framework, the lack of behavioural data may affect interpretability of the clinical meaningfulness of the data (as only the SPRS was used to measure general lifestyle changes, not specific outcomes). For example, this includes (1) how the range of differences in number of affected tracts may be related to the degree of clinical disability and; (2) how a specific tract injury may be linked to deficits in cognitive, motor, psychological, or social outcomes. Linking white matter profiles to clinical profiles may also provide added value for personalised training and is therefore an important step to translate the basic science into the clinical practice. This may eventually lead to tailored training programs with details provided at baseline or at the end of a training protocol, leading to the potential for better health care options for heterogeneous populations.

4.4. Conclusion

This study presents a novel *individualised profiling* framework that, for the first time, implements TractLearn in m-sTBI patients to detect the location and extent of fibre density loss in all tracts across the brain, combined with an analysis of tract-wide density loss in those damaged tracts. This approach captures the heterogeneity within individual m-sTBI patients and can therefore be very useful in clinically heterogeneous populations. This study extends on the recent papers on single-subject profiling (Attyé et al., 2021; Chamberland et al., 2021; Jolly et al., 2020; Lv et al., 2021) by developing further insight into damaged tracts, as well as using specific FBA-framework based FD measures. With further validation of this approach, single-subject profiles may eventually assist clinicians with more quantitative information about the changes in the brain structure, potentially augmenting diagnostic and/or treatment decisions made with respect to individual patients with m-sTBI.

Funding

Karen Caeyenberghs: Australian Catholic University Research Fund [#902915] and National Health and Medical Research Council [#APP1143816]. Govinda Poudel: Australian Catholic University Research Fund. Peter H Wilson: Australian Catholic University Research Centre Scheme.

CRediT authorship contribution statement

Adam Clemente: Conceptualization, Methodology, Software, Formal analysis, Investigation, Data curation, Writing – original draft, Writing – review & editing, Visualization. **Arnaud Attyé:** Software, Formal analysis, Investigation, Data curation, Writing – original draft, Writing – review & editing, Visualization. **Félix Renard:** Software, Formal analysis, Investigation, Data curation, Writing – review & editing. **Fernando Calamante:** Conceptualization, Methodology, Software, Formal analysis, Investigation, Data curation, Writing – review & editing. **Alex Burmester:** Software, Formal analysis, Investigation, Data curation, Writing – original draft, Writing – review & editing, Visualization. **Phoebe Imms:** Investigation, Resources, Data curation, Writing – review & editing. **Evelyn Deutscher:** Formal analysis, Writing – review & editing. **Hamed Akhlaghi:** Resources, Data curation. **Paul Beech:** Formal analysis, Writing – review & editing. **Peter H Wilson:** Conceptualization, Resources, Writing – review & editing, Supervision, Funding acquisition. **Govinda Poudel:** Conceptualization, Methodology, Software, Validation, Formal analysis, Resources, Data curation,

Writing – review & editing, Visualization, Supervision. **Juan F. Domínguez D:** Conceptualization, Methodology, Software, Validation, Formal analysis, Resources, Data curation, Writing – review & editing, Supervision. **Karen Caeyenberghs:** Conceptualization, Methodology, Validation, Formal analysis, Investigation, Resources, Writing – original draft, Writing – review & editing, Supervision, Project administration, Funding acquisition.

Declaration of Competing Interest

The authors declare that they have no known competing financial interests or personal relationships that could have appeared to influence the work reported in this paper.

Data availability

Data will be made available on request.

Acknowledgement

We would like to thank Michael Kean and the radiographers at the Royal Children's Hospital. We would also like to thank Laura Dal Pozzo for assistance with figure construction.

References

Adams, J. H., Doyle, D., Ford, I., Gennarelli, T. A., Graham, D. I., & McLellan, D. R. (1989). Diffuse axonal injury in head injury: definition, diagnosis and grading. Histopathology, 15(1), 49-59. 1 0.1111/j.1365-2559.1989.tb03040.x.

Andersson, J.L., Sotiropoulos, S.N., 2016. An integrated approach to correction for off-resonance effects and subject movement in diffusion MR imaging. Neuroimage 125, 1063–1078. https://doi.org/10.1016/j.neuroimage.2015.10.019.

Andersson, J.L., Graham, M.S., Zsoldos, E., Sotiropoulos, S.N., 2016. Incorporating outlier detection and replacement into a non-parametric framework for movement and distortion correction of diffusion MR images. Neuroimage 141, 556–572. https://doi.org/10.1016/j.neuroimage.2016.06.058.

Attye, A., Renard, F., Baciu, M., Roger, E., Lamalle, L., Dehail, P., et al. (2021). TractLearn: a geodesic learning framework for quantitative analysis of brain bundles. Neuroimage, 233, 117927 10.1101/2020.05.27.20113027.

Caeyenberghs, K., Leemans, A., Coxon, J., Leunissen, I., Drijkoningen, D., Geurts, M., Gooijers, J., Michiels, K., Sunaert, S., Swinnen, S.P., 2011. Bimanual coordination and corpus callosum microstructure in young adults with traumatic brain injury: a diffusion tensor imaging study. J. Neurotrauma 28 (6), 897–913.

Cetin Karayumak, S., Bouix, S., Ning, L., James, A., Crow, T., Shenton, M., Kubicki, M., Rathi, Y., 2019. Retrospective harmonization of multi-site diffusion MRI data acquired with different acquisition parameters. Neuroimage 184, 180–200.

Chamberland, M., Genc, S., Tax, C.M.W., Shastin, D., Koller, K., Raven, E.P., Cunningham, A., Doherty, J., van den Bree, M.B.M., Parker, G.D., Hamandi, K., Gray, W.P., Jones, D.K., 2021. Detecting microstructural deviations in individuals with deep diffusion MRI tractometry. Nature Comput. Sci. 1 (9), 598–606.

Dadas, A., Washington, J., Diaz-Arrastia, R., Janigro, D., 2018. Biomarkers in traumatic brain injury (TBI): a review. Neuropsychiatr. Dis. Treat. 14, 2989. https://doi.org/10.2147/NDT.S125620.

Dennis, E.L., Caeyenberghs, K., Hoskinson, K.R., Merkley, T.L., Suskauer, S.J., Asarnow, R.F., Babikian, T., Bartnik-Olson, B., Bickart, K., Bigler, E.D., Ewing-Cobbs, L., Figaji, A., Giza, C.C., Goodrich-Hunsaker, N.J., Hodges, C.B., Hovenden, E. S., Irimia, A., Königs, M., Levin, H.S., Lindsey, H.M., Max, J.E., Newsome, M.R., Olsen, A., Ryan, N.P., Schmidt, A.T., Spruiell, M.S., Wade, B.S.C., Ware, A.L., Watson, C.G., Wheeler, A.L., Yeates, K.O., Zielinski, B.A., Kochunov, P., Jahanshad, N., Thompson, P.M., Tate, D.F., Wilde, E.A., 2021. White matter disruption in pediatric traumatic brain injury: results from enigma pediatric moderate to severe traumatic brain injury. Neurology 97 (3), e298–e309.

Dewan, M. C., Rattani, A., Gupta, S., Baticulon, R. E., Hung, Y. C., Punchak, M., … & Park, K. B. (2018). Estimating the global incidence of traumatic brain injury. J. Neurosurgery, 130(4), 1080-1097. 10.23736/S0390-5616.18.04532-0.

Dhollander, T., & Connelly, A. (2016). A novel iterative approach to reap the benefits of multi-tissue CSD from just single-shell (+b=0) diffusion MRI data. In: Proceedings of the International Society for Magnetic Resonance in Medicine, 3010.

Dhollander, T., Raffelt, D., & Connelly, A. (2016). Unsupervised 3-tissue response function estimation from single-shell or multi-shell diffusion MR data without a co-registered T1 image. ISMRM Workshop on Breaking the Barriers of Diffusion MRI, 5.

Dhollander, T., Mito, R., Raffelt, D., & Connelly, A. (2019). Improved white matter response function estimation for 3-tissue constrained spherical deconvolution. In: Proceedings of the International Society for Magnetic Resonance in Medicine, 555.

Dhollander, T., Clemente, A., Singh, M., Boonstra, F., Civier, O., Dominguez, D.J., et al., 2021. Fixel-based analysis of diffusion MRI: methods, applications, challenges and opportunities. Neuroimage 241, 118417. https://doi.org/10.1016/j.neuroimage.2021.118417.

Dyrby, T.B., Lundell, H., Burke, M.W., Reislev, N.L., Paulson, O.B., Ptito, M., Siebner, H. R., 2014. Interpolation of diffusion weighted imaging datasets. Neuroimage 103, 202–213. https://doi.org/10.1016/j.neuroimage.2014.09.005.

Egorova, N., Dhollander, T., Khlif, M.S., Khan, W., Werden, E., Brodtmann, A., 2020. Pervasive white matter fiber degeneration in ischemic stroke. Stroke 51 (5), 1507–1513. https://doi.org/10.1161/STROKEAHA.119.028143.

Frank, L.R., 2001. Anisotropy in high angular resolution diffusion-weighted MRI. Magn. Reson. Med. 45 (6), 935–939. https://doi.org/10.1002/mrm.1125.

Gajamange, S., Raffelt, D., Dhollander, T., Lui, E., van der Walt, A., Kilpatrick, T., Fielding, J., Connelly, A., Kolbe, S., 2018. Fibre-specific white matter changes in multiple sclerosis patients with optic neuritis. NeuroImage: Clinical 17, 60–68.

Genc, S., Tax, C.M.W., Raven, E.P., Chamberland, M., Parker, G.D., Jones, D.K., 2020. Impact of b-value on estimates of apparent fibre density. Hum. Brain Mapp. 41 (10), 2583–2595. https://doi.org/10.1002/hbm.24964.

Gottlieb, E., Egorova, N., Khlif, M.S., Khan, W., Werden, E., Pase, M.P., Brodtmann, A., 2020. Regional neurodegeneration correlates with sleep-wake dysfunction after stroke. Sleep 43 (9), zsaa054. https://doi.org/10.1093/sleep/zsaa054.

Grech-Sollars, M., Hales, P.W., Miyazaki, K., Raschke, F., Rodriguez, D., Wilson, M., Gill, S.K., Banks, T., Saunders, D.E., Clayden, J.D., Gwilliam, M.N., Barrick, T.R., Morgan, P.S., Davies, N.P., Rossiter, J., Auer, D.P., Grundy, R., Leach, M.O., Howe, F. A., Peet, A.C., Clark, C.A., 2015. Multi-centre reproducibility of diffusion MRI parameters for clinical sequences in the brain. NMR Biomed. 28 (4), 468–485.

Han, K., Davis, R.A., Chapman, S.B., Krawczyk, D.C., 2017. Strategy-based reasoning training modulates cortical thickness and resting-state functional connectivity in adults with chronic traumatic brain injury. Brain and Behaviour 7 (5), 1–27. https://doi.org/10.1002/brb3.687.

Imms, P., Clemente, A., Deutscher, E., Radwan, A. M., Akhlaghi, H., Beech, P., Wilson, P. H., Irimia, A., Poudel, G., Domínguez D, J. F., & Caeyenberghs, K. (2022). Personalised structural connectomics for moderate-to-severe traumatic brain injury. Network Neurosci. 10.1101/2022.03.02.22271654.

James, S.L., Theadom, A., Ellenbogen, R.G., Bannick, M.S., Montjoy-Venning, W., Lucchesi, L.R., et al., 2019. Global, regional, and national burden of traumatic brain injury and spinal cord injury, 1990–2016: a systematic analysis for the Global Burden of Disease Study 2016. The Lancet Neurology 18 (1), 56–87.

Jolly, A.E., Bălăeț, M., Azor, A., Friedland, D., Sandrone, S., Graham, N.S., Sharp, D.J., 2020. Detecting axonal injury in individual patients after traumatic brain injury. Brain awaa372. https://doi.org/10.1093/brain/awaa372.

Kellner, E., Dhital, B., Kiselev, V.G., Reisert, M., 2016. Gibbs-ringing artifact removal based on local subvoxel-shifts. Magn. Reson. Med. 76 (5), 1574–1581. https://doi.org/10.1002/mrm.26054.

Koliatsos, V.E., Alexandris, A.S., 2019. Wallerian degeneration as a therapeutic target in traumatic brain injury. Curr. Opin. Neurol. 32 (6), 786. https://doi.org/10.1097/WCO.0000000000000763.

Leemans, A., Jeurissen, B., Sijbers, J., & Jones, D. K. (2009). ExploreDTI: A graphical toolbox for processing, analyzing, and visualizing diffusion MR data. In: Proceedings of the International Society for Magnetic Resonance in Medicine, 17(1).

Liang, X., Yeh, C. H., Poudel, G., Swinnen, S. P., & Caeyenberghs, K. (2021). Longitudinal fixel-based analysis reveals restoration of white matter alterations following balance training in young brain-injured patients. NeuroImage: Clinical, 30, 102621. 10.1016/j.nicl.2021.102621.

Liew, S.L., Zavaliangos-Petropulu, A., Jahanshad, N., Lang, C.E., Hayward, K.S., Lohse, K. R., Thompson, P.M., 2022. The ENIGMA Stroke Recovery Working Group: Big data neuroimaging to study brain–behavior relationships after stroke. Hum. Brain Mapp. 43 (1), 129–148. https://doi.org/10.1002/hbm.25015.

Lv, J., Di Biase, M., Cash, R.F.H., Cocchi, L., Cropley, V.L., Klauser, P., Tian, Y.e., Bayer, J., Schmaal, L., Cetin-Karayumak, S., Rathi, Y., Pasternak, O., Bousman, C., Pantelis, C., Calamante, F., Zalesky, A., 2021. Individual deviations from normative models of brain structure in a large cross-sectional schizophrenia cohort. Mol. Psychiatry 26 (7), 3512–3523.

Maas, A.I.R., Menon, D.K., Manley, G.T., Abrams, M., Åkerlund, C., Andelic, N., et al., 2022. Traumatic brain injury: progress and challenges in prevention, clinical care, and research. The Lancet Neurology 21 (11), 1004–1060.

Mirzaalian, H., Ning, L., Savadjiev, P., Pasternak, O., Bouix, S., Michailovich, O., et al., 2016. Inter-site and inter-scanner diffusion MRI data harmonization. Neuroimage 135, 311–323.

Mito, R., Raffelt, D., Dhollander, T., Vaughan, D. N., Tournier, J. D., Salvado, O., et al. (2018). Fibre-specific white matter reductions in Alzheimer's disease and mild cognitive impairment. Brain, 141(3), 888-902. 10.1093/brain/awx355.

Oldfield, R.C., 1971. The assessment and analysis of handedness: The Edinburgh inventory. Neuropsychologia 9 (1), 97–113. https://doi.org/10.1016/0028-3932(71)90067-4.

Olsen, A., Babikian, T., Bigler, E.D., Caeyenberghs, K., Conde, V., Dams-O'Connor, K., et al., 2021. Toward a global and reproducible science for brain imaging in neurotrauma: the ENIGMA adult moderate/severe traumatic brain injury working group. Brain Imaging Behav. 15 (2), 526–554.

Poudel, G.R., Dominguez D, J.F., Verhelst, H., Vander Linden, C., Deblaere, K., Jones, D. K., et al., 2020. Network diffusion modeling predicts neurodegeneration in traumatic brain injury. Ann. Clin. Transl. Neurol. 7 (3), 270–279.

Rabinowitz, A.R., Levin, H.S., 2014. Cognitive sequelae of traumatic brain injury. Psychiatr. Clin. N. Am. 37 (1), 1–11.

Raffelt, D.A., Smith, R.E., Ridgway, G.R., Tournier, J.-D., Vaughan, D.N., Rose, S., et al., 2015. Connectivity-based fixel enhancement: whole-brain statistical analysis of diffusion MRI measures in the presence of crossing fibres. Neuroimage 117, 40–55.

Raffelt, D., Tournier, J.D., Fripp, J., Crozier, S., Connelly, A., Salvado, O., 2011. Symmetric diffeomorphic registration of fibre orientation distributions. Neuroimage 56 (3), 1171–1180. https://doi.org/10.1016/j.neuroimage.2011.02.014.

Raffelt, D., Tournier, J.D., Crozier, S., Connelly, A., Salvado, O., 2012. Reorientation of fibre orientation distributions using apodized point spread functions. Magn. Reson. Med. 67 (3), 844–855. https://doi.org/10.1002/mrm.23058.

Raffelt, D.A., Tournier, J.D., Smith, R.E., Vaughan, D.N., Jackson, G., Ridgway, G.R., Connelly, A., 2017. Investigating white matter fibre density and morphology using fixel-based analysis. Neuroimage 144 (A), 58–73. https://doi.org/10.1016/j.neuroimage.2016.09.029.

Roberts, R.E., Anderson, E.J., Husain, M., 2013. White matter microstructure and cognitive function. Neuroscientist 19 (1), 8–15. https://doi.org/10.1177/1073858411421218.

Scarpazza, C., Ha, M., Baecker, L., Garcia-Dias, R., Pinaya, W.H.L., Vieira, S., Mechelli, A., 2020. Translating research findings into clinical practice: a systematic and critical review of neuroimaging-based clinical tools for brain disorders. Transl. Psychiatry 10 (1), 1–16. https://doi.org/10.1038/s41398-020-0798-6.

Schmeel, F.C., 2019. Variability in quantitative diffusion-weighted MR imaging (DWI) across different scanners and imaging sites: is there a potential consensus that can help reducing the limits of expected bias? Eur. Radiol. 29, 2243–2245. https://doi.org/10.1007/s00330-018-5866-4.

Strangman, G.E., O'Neil-Pirozzi, T.M., Supelana, C., Goldstein, R., Katz, D.I., Glenn, M.B., 2010. Regional brain morphometry predicts memory rehabilitation outcome after traumatic brain injury. Front. Hum. Neurosci. 4, 182. https://doi.org/10.3389/fnhum.2010.00182.

Tate, R.L., Simpson, G.K., Soo, C.A., Lane-Brown, A.T., 2011. Participation after acquired brain injury: clinical and psychometric considerations of the Sydney Psychosocial Reintegration Scale (SPRS). J. Rehabil. Med. 43 (7), 609–618. https://doi.org/10.2340/16501977-0829.

Tax, C.MW., Grussu, F., Kaden, E., Ning, L., Rudrapatna, U., John Evans, C., St-Jean, S., Leemans, A., Koppers, S., Merhof, D., Ghosh, A., Tanno, R., Alexander, D.C., Zappalà, S., Charron, C., Kusmia, S., Linden, D.EJ., Jones, D.K., Veraart, J., 2019. Cross-scanner and cross-protocol diffusion MRI data harmonisation: a benchmark database and evaluation of algorithms. Neuroimage 195, 285–299.

Teasdale, G., Jennett, B., 1974. Assessment of coma and impaired consciousness: a practical scale. Lancet 304 (7872), 81–84. https://doi.org/10.1016/S0140-6736(74)91639-0.

Tournier, J. D., Smith, R., Raffelt, D., Tabbara, R., Dhollander, T., Pietsch, M., et al. (2019). MRtrix3: A fast, flexible and open software framework for medical image processing and visualisation. *Neuroimage, 202,* 116137. 10.1016/j.neuroimage.2019.116137.

Veraart, J., Novikov, D.S., Christiaens, D., Ades-Aron, B., Sijbers, J., Fieremans, E., 2016. Denoising of diffusion MRI using random matrix theory. Neuroimage 142, 394–406. https://doi.org/10.1016/j.neuroimage.2016.08.016.

Verdi, S., Marquand, A.F., Schott, J.M., Cole, J.H., 2021. Beyond the average patient: how neuroimaging models can address heterogeneity in dementia. Brain 144 (10), 2946–2953. https://doi.org/10.1093/brain/awab165.

Verhelst, H., Giraldo, D., Vander Linden, C., Vingerhoets, G., Jeurissen, B., Caeyenberghs, K., 2019. Cognitive training in young patients with traumatic brain injury: a fixel-based analysis. Neurorehabil. Neural Repair 33 (10), 813–824. https://doi.org/10.1177/1545968319868720.

Volovici, V., Bruggeman, G.F., Haitsma, I.K., 2021. MRI studies of traumatic axonal injury: still a long way to go—misuse of the Adams classification. Acta Neurochir. 163 (5), 1445–1446. https://doi.org/10.1007/s00701-021-04757-8.

Wallace, E.J., Mathias, J.L., Ward, L., 2018. The relationship between diffusion tensor imaging findings and cognitive outcomes following adult traumatic brain injury: a meta-analysis. Neurosci. Biobehav. Rev. 92, 93–103. https://doi.org/10.1016/j.neubiorev.2018.05.023.

Wasserthal, J., Neher, P., Maier-Hein, K.H., 2018. Tractseg-fast and accurate white matter tract segmentation. Neuroimage 183, 239–253. https://doi.org/10.1016/j.neuroimage.2018.07.070.

Wasserthal, J., Neher, P.F., Hirjak, D., Maier-Hein, K.H., 2019. Combined tract segmentation and orientation mapping for bundle-specific tractography. Med. Image Anal. 58, 101559 https://doi.org/10.1016/j.media.2019.101559.